

Copper oxidation state in chalcopyrite: Mixed Cu d^9 and d^{10} characteristics

C.I. Pearce^a, R.A.D. Patrick^{a,*}, D.J. Vaughan^a, C.M.B. Henderson^{a,b}, G. van der Laan^{a,b}

^a School of Earth, Atmospheric and Environmental Sciences and Williamson Research Centre for Molecular Environmental Science,
University of Manchester, Manchester M13 9PL, UK

^b CCLRC Daresbury Laboratory, Warrington WA4 4AD, UK

Received 22 December 2005; accepted in revised form 23 May 2006

Abstract

The determination of the oxidation states of copper and iron in sulfides, and chalcopyrite (CuFeS_2) in particular, using $2p$ X-ray photoemission spectroscopy (XPS) and $L_{2,3}$ -edge X-ray absorption spectroscopy (XAS) is revisited. Reassessment of the published spectra derived by these methods produces consistent results and reveals the ‘ d count’ in the copper compounds to be intermediate between d^9 and d^{10} . Nevertheless, these covalent copper compounds can be divided into those nominally monovalent and those nominally divalent. The Fe $L_{2,3}$ -edge XAS of chalcopyrite, along with Mössbauer data, confirm the presence of high-spin Fe^{3+} . Chalcopyrite, despite recent published reports to the contrary, clearly belongs to the monovalent copper class.

© 2006 Elsevier Inc. All rights reserved.

1. Introduction

The oxidation state of metals in sulfides has been extensively studied in order to understand their fundamental crystal chemical properties and the processes of mineral formation and breakdown, mineral processing, and the role of sulfides in environmental pollution. A wide range of spectroscopies have been employed in these investigations, many of which have been focussed on phases in the Cu–Fe–S system because of the common occurrence of two valence states in nature for both copper ($\text{Cu}^+/\text{Cu}^{2+}$) and iron ($\text{Fe}^{2+}/\text{Fe}^{3+}$). In particular, the bulk and surface properties of chalcopyrite (CuFeS_2), the world’s most important source of copper, have been studied. Chalcopyrite crystallises in the tetragonal space group $I\bar{4}2d$ and has a zincblende structure with four-coordinate cations and anions forming distinct corner-sharing tetrahedra. Cu and Fe are ordered into alternate cation sites. It is a semiconductor in which the oxidation states of Cu and Fe have

been regarded generally as represented by formal valencies of $\text{Cu}^+\text{Fe}^{3+}\text{S}_2^{2-}$, supported by a diverse body of experimental evidence. However, this has been challenged in recent publications (Todd and Sherman, 2003; Todd et al., 2003; Mikhlin et al., 2005) which have proposed valencies of $\text{Cu}^{2+}\text{Fe}^{2+}\text{S}_2^{2-}$ on the basis of X-ray absorption spectroscopic (XAS) evidence. This paper demonstrates that Cu in CuFeS_2 is indeed nominally monovalent and that Fe is nominally trivalent, and it is also shown that assigning formal valence states to covalent copper sulfides is an oversimplification.

Much of the recent spectroscopic evidence confirming that the oxidation state of copper in chalcopyrite (and in almost all other Cu-sulfide minerals) is Cu(I) comes from Cu $L_{3,2}$ -edge XAS studies (Grioni et al., 1989, 1992; van der Laan et al., 1992, 2002), the results for which are in agreement with those from the Cu $2p$ X-ray photoemission spectroscopy (XPS) work of Nakai et al. (1978). However, a minor amount of Cu(II) has been detected in metastable synthetic tetrahedrite ($\text{Cu}_{12+x}\text{Sb}_{4+y}\text{S}_{13}$) as a charge balancing component (Patrick et al., 1993). The interpretation of the XAS spectra depends crucially on the peaks

* Corresponding author. Fax: +44 0161 275 3947.

E-mail address: richard.patrick@manchester.ac.uk (R.A.D. Patrick).

being assigned correctly. In particular, the small separation of the energies between the main peak in the spectra of Cu(II)-oxides and sulfides (930.5–931.2 eV) compared to the first peak in Cu(I)-oxides and sulfides (931.9–932.5 eV) means that these assignments require extreme care. (Note that the Cu(II) peak in the sulfide tetrahedrite is at 930.7 eV and the Cu(I) peak in Cu₂O is at 933.4 eV.) Energy calibration of experimental spectra using known standards is essential to allow comparisons with other published data, and to prevent the misinterpretation of data based on inaccurate energy positions. Recommended calibration values are 931.2 eV for the Cu *L*₃ peak in CuO and 707.7 eV for the Fe *L*₃ peak in Fe metal. All theoretical and experimental investigations recognise the covalent character of chalcopyrite which involves extensive overlapping of Cu and Fe metal *d* orbitals across the whole valence band (Tossell et al., 1982; Kurmaev et al., 1998; Edelbro et al., 2003).

Surface oxidation is a particular characteristic of copper sulfides which can produce peaks that might be attributed to the ‘bulk’ spectrum. Relatively less severe surface oxidation of CuFeS₂ leads to the production of Cu(I) sulfide species such as CuS, Cu_{1-x}S, Cu_{1-x}Fe_{1-y}S and CuS₂, that overlie metal-depleted surface layers (Vaughan et al., 1995; Yin et al., 2000; Mikhlin et al., 2004). XPS analysis of these surface copper sulfide species reveals no change in the binding energy of the Cu 2*p*_{3/2} spectra: the shake-up satellites in the spectra at 940–945 eV, characteristic of Cu(II) species, are absent indicating that the Cu–S sulfides and the metal-deficient surface layers retain their Cu(I) character, even after this moderate oxidation (Vaughan et al., 1995; Yin et al., 2000; Mikhlin et al., 2004). Cu(II)–O species such as CuO, Cu(OH)₂ and Cu₃(SO₄)(OH)₄ are produced by more extensive oxidation of chalcopyrite (Velasquez et al., 2001). As the Cu(II) *L*₃ XAS peak is 25 times more intense than that of the Cu(I) peak (Patrick et al., 1993), very small amounts of a Cu(II) phase can produce very significant peaks around 931 eV, which may be observed in the bulk spectrum. Furthermore, XPS data are dominated by the signal from the top few atomic layers of the sample surface (~5 Å for XPS versus ~50 Å for XAS), making the data highly sensitive to the effects of alteration, such as surface oxidation.

CuFeS₂ is an antiferromagnetic semiconductor and numerous Mössbauer spectra recorded from the iron in chalcopyrite (see Vaughan and Craig (1978) and references therein) reveal it to be “magnetically coupled high-spin Fe³⁺”. This finding, combined with the lack of an observable magnetic moment on the Cu atom in neutron diffraction experiments (Donnay et al., 1958), clearly supports a formal Cu⁺Fe³⁺S₂²⁻ configuration.

In mineralogical and geochemical studies, simple oxidation states of Cu⁺ or Cu²⁺ and Fe²⁺ or Fe³⁺ are generally assumed. ‘Truly’ monovalent copper has a completely filled *d*-electron shell (*d*¹⁰) while divalent copper has only nine *d*-electrons (*d*⁹). However, in covalent or metallic/semimetallic materials, such as metal sulfides, it is quite possible for the

d-count to be a non-integral value. In such cases, the question of whether Cu is present as 1⁺ or 2⁺ is an oversimplification and the Cu valency should be assigned as nominally monovalent or nominally divalent. It is difficult to give an absolute number for the *d*-count, since this will depend on the extent to which the electron density is localised on particular atoms or delocalised into the chemical bonds between these atoms. For instance, in a model calculation, the computed *d*-count will depend on the size of the chosen atomic sphere: in an experimental measurement, it will depend partly on the nature of the experimental probe. The difficult task of determining the *d* count becomes easier if data acquired for a material such as chalcopyrite are compared with those for model compounds such as CuO and Cu₂O which can be used as examples of typically divalent and monovalent copper compounds, respectively. These compounds also have the advantage that they have been well studied but both compounds have *d*-counts that are significantly different from *d*^{9.0} and *d*^{10.0}. Core-level spectroscopies, such as 2*p* X-ray photoemission (XPS) and *L*_{2,3} X-ray absorption spectroscopy (XAS), provide powerful methods to determine the *d*-count and, hence, the valence states of 3*d* transition-metal ions. Both of these methods give a division of Cu compounds and minerals into two different classes. These two classes can be assigned to formally divalent and formally monovalent Cu compounds, and the assignment for each Cu compound is consistently the same for both XPS and XAS data. As explained below, it is clear that chalcopyrite is in the monovalent Cu class.

2. Data collection

The Cu 2*p* XPS data presented here (Fig. 1) are from Fujisawa et al. (1994) and experimental details are provided in that publication. The XAS *L*-edge spectra provided here (Figs. 2 and 3) were collected at the Synchrotron Radiation Source at CCLRC, Daresbury Laboratory, apart from the potassium thioferrite spectrum which is from Atanasov et al. (1995). The Cu *L*_{2,3}-edge spectra were obtained on experimental station 3.4, and the Fe *L*_{2,3}-edge spectra on stations 1.1 and 5U. The experimental details are presented in van der Laan et al. (1992) (Cu *L*-edge) and Patrick et al. (2002) (Fe *L*-edge). The energy calibrations for the copper spectra presented in Fig. 2 are based on a Cu *L*₃ peak energy for CuO of 931.2 ± 0.05 eV. The energy calibration of Fe *L*-edge spectra presented in Fig. 3 was undertaken using the Fe *L*₃ peak of Fe metal, assuming a photon energy of 707.7 eV for pure Fe (Chen et al., 1995). Standards were measured at the beginning and end of each sample batch.

The iron Mössbauer data reported here are as originally presented by Vaughan and Burns (1972) using experimental methods as originally described in Vaughan and Ridout (1971). Isomer shift values are quoted (in mm s⁻¹) against the centre of gravity of the spectrum of iron foil as zero.

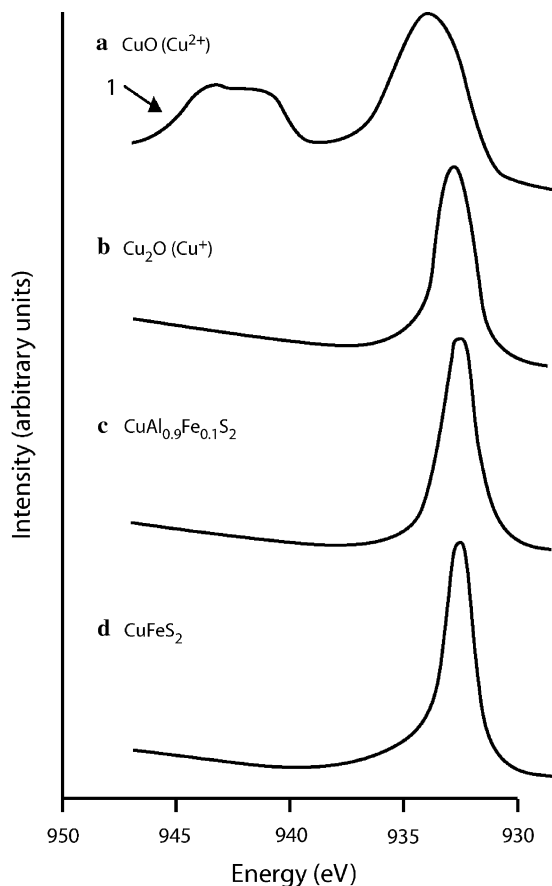


Fig. 1. Cu $2p_{3/2}$ XPS of reference materials with formal valences (a) Cu^{2+} (CuO) and (b) Cu^+ (Cu_2O) (redrawn from Fujisawa et al., 1994) compared with the Cu $2p$ XPS spectra of (c) $\text{CuAl}_{0.9}\text{Fe}_{0.1}\text{S}_2$ (redrawn from Fujisawa et al., 1994) and (d) CuFeS_2 . Peak 1 shows the satellite in a nominally divalent mineral, CuO.

3. Results

3.1. Cu $2p$ X-ray photoemission

The Cu $2p$ XPS spectra for divalent compounds have a strong satellite structure at typically 7–10 eV above the main peak (peak 1, Fig. 1a), and this satellite peak is not observed in monovalent compounds (Figs. 1b, c and d). While the main peak is a single line with primarily $2p3d^{10}\underline{L}$ character, the satellite has a characteristic multiplet structure with mainly $2p3d^9$ character (van der Laan et al., 1981). In this notation, $2p$ and \underline{L} indicate a hole in the core and ligand shell, respectively. The higher energy of the satellite is due to the Coulomb repulsion between the core hole and the $3d$ hole. In other words, the atomic d^{10} state is pulled down by the local Coulomb potential of the core hole. While the satellite ($2p3d^9$) peak is roughly at a fixed position, the main ($2p3d^{10}\underline{L}$) peak shifts according to the electronegativity of the effective ligand field around the Cu atom. The XPS spectra for $\text{Cu}^+\text{Al}_{0.9}^{3+}\text{Fe}_{0.1}^{3+}\text{S}_2^{2-}$ (Fig. 1c) and $\text{Cu}^+\text{Fe}^{3+}\text{S}_2^{2-}$ (Fig. 1d) show no evidence of a satellite structure and strongly resemble the spectrum for monovalent Cu_2O .

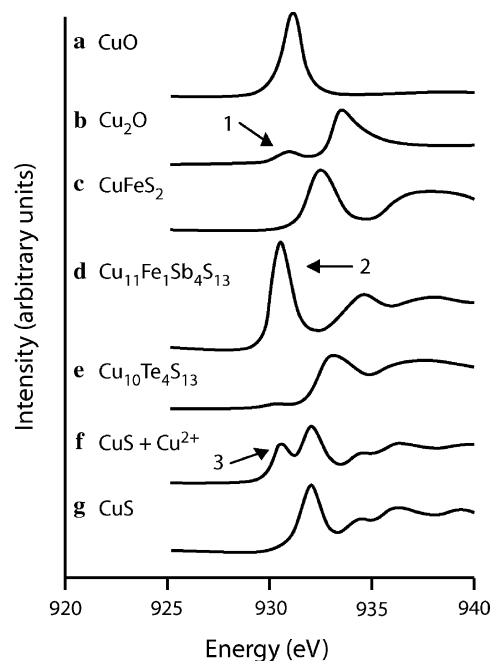


Fig. 2. Cu L_3 edge XAS spectra of selected Cu compounds. (a) CuO, N.B. the intensity is reduced by 25x; (b) Cu_2O with a very minor Cu^{2+} component (peak 1); (c) CuFeS_2 ; (d) $\text{Cu}_{11}\text{Fe}_1\text{Sb}_4\text{S}_{13}$ tetrahedrite with a component of Cu^{2+} (peak 2); (e) $\text{Cu}_{10}\text{Te}_4\text{S}_{13}$ goldfieldite; (f) CuS with Cu^{2+} contamination (peak 3); and (g) CuS pure.

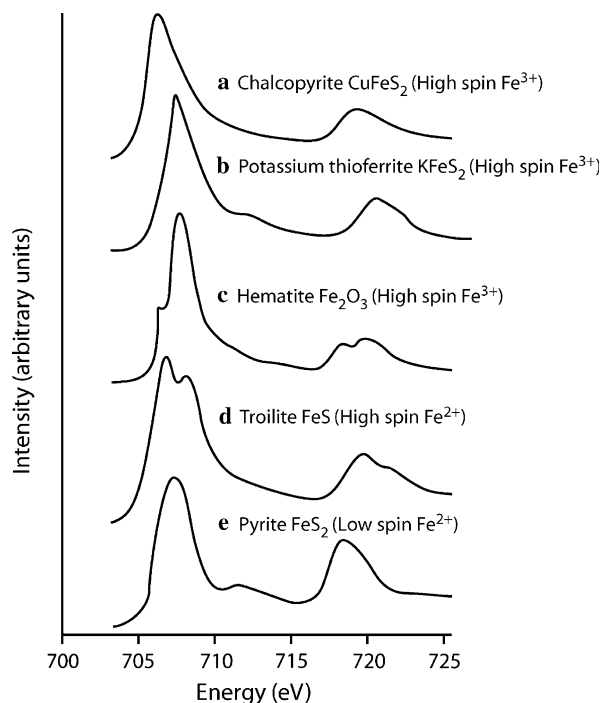


Fig. 3. Experimental Fe $L_{2,3}$ XAS spectra for (a) chalcopyrite CuFeS_2 , (b) potassium thioferrite KFeS_2 , (redrawn from Atanasov et al., 1995), N.B. energy not calibrated but included to demonstrate spectral shape, (c) hematite Fe_2O_3 , (d) troilite FeS and (e) pyrite FeS_2 .

The energy positions of the main ($2p_{3/2}3d^{10}\underline{L}$) peak for various Cu compounds are given in Table 1; note that the electronegativity decreases for the different compounds

Table 1

Energy position (eV) of the Cu $2p_{3/2}$ XPS main ($\underline{2p_{3/2}3d^{10}L}$) peak and assigned d count, n_d for various monovalent and divalent Cu compounds (Folmer and Jellinek, 1980; van der Laan et al., 1981; Shen et al., 1987; Tjeng, 1990; Fujisawa et al., 1994)

Compound	XPS main peak (eV)	n_d
CuF ₂	936.6	9.19
CuCl ₂	934.6	9.31
CuO	933.2	9.44
CuBr ₂	933.1	9.45
Cu ₂ O	932.4	>9.5
CuFeS ₂	932.3	>9.5
Cu ₂ S	932.0	>9.5
CuS	931.4	>9.5
CuS ₂	931.3	>9.5

For $n_d > 9.5$ the satellite intensity becomes too small to give a more precise value for n_d .

from the top to the bottom of the table. If the electronic charge on the Cu atom is reduced, the electrostatic potential is lowered and the binding energy of the core electron is increased (Karlsson et al., 1992a). The energy position of CuFeS₂ is at about the same position as Cu₂O, hence the electronic charge on the Cu will be similar in these two phases.

Using a simple and well-tested model for Cu $2p$ XPS it is possible to estimate the number of d electrons, n_d , by using the satellite intensity and the energy separation between the satellite and main peak (van der Laan et al., 1981). Results from different sources (Folmer and Jellinek, 1980; van der Laan et al., 1981; Shen et al., 1987; Tjeng, 1990; Fujisawa et al., 1994) are listed in Table 1, where the different studies use the same analysis so that the n_d values can be compared to each other. However, the calculation based on an impurity Anderson model without multiplet structure (Karlsson et al., 1992b) gives somewhat different n_d values of 9.25 for CuO and 9.42 for Cu₂O. Nevertheless, the overall trend of n_d with electronegativity is very similar to that shown in Table 1. The difference in the intensity of the d^p satellite in Cu₂O (Fig. 1b) compared to CuO (Fig. 1a) is only partly due to the larger $3d$ occupancy, which favours a larger main (d^{10}) peak in Cu₂O, and partly due to the stronger coupling in the final state for Cu₂O. Since the main coupling in Cu₂O is due to electron hopping into the conduction state, the electron can have any quantum number and the coupling is very efficient. In CuO, on the other hand, the main coupling is due to a valence electron hopping into a $3d$ hole. Since the quantum number of the $3d$ hole is fixed, the hopping can only take place for one specific value of the quantum number of the valence electron. As a result the coupling is weaker for CuO, and the transfer of intensity from the satellite to the main peak is smaller.

The satellite intensity in XPS increases with the number of d holes; however, it is by no means linearly proportional. When the number of d holes is small (that is, $n_d > 9.5$), the satellite intensity remains low but increases rather rapidly with an increasing number of d holes ($n_d < 9.5$). Thus despite the various parameters involved, such as symmetry,

hybridization and Coulomb interaction, the presence (or absence) of the satellite peak is a good indication of whether a Cu compound is divalent (or monovalent). Since the satellite intensity is very low for monovalent compounds, the d -count is not specified in this case in Table 1. The fact that the d -count is always quite far from d^{10} is due to the covalent character of the compounds as confirmed by the results of bandstructure calculations (Hamajima et al., 1981; Kurmaev et al., 1998; Edelbro et al., 2003). For instance, the calculation by Hamajima et al. (1981) quotes values for Cu in CuFeS₂ of $n_d = 9.63$, $n_{4s} = 0.54$ and $n_{4p} = 0.76$. The oxidation states are therefore not mixed Cu⁺ and Cu²⁺ (d^9 and d^{10}) but are in fact intermediate in character, reflecting the extent to which materials such as chalcopyrite differ from truly ‘ionic’ solids and the electrons are delocalised, as in a metal.

3.2. Fe $2p$ X-ray photoemission

Analysis of the Fe $2p$ XPS in CuFeS₂ by Fujisawa et al. (1994) suggests a net Fe d -electron number of 4.6 ± 0.1 with a Fe magnetic moment of $3.8 \mu_B$, which is in agreement with the experimental value of $3.85 \pm 0.20 \mu_B$ obtained by Donnay et al. (1958).

3.3. Cu L_3 XAS

The experimental Cu L_3 XAS data for chalcopyrite in the literature (Grioni et al., 1989; van der Laan et al., 1992; Patrick et al., 1993; Mikhlin et al., 2004) are in good agreement and, for localised $3d^n$ configurations, the L_3 XAS offers the unique possibility of determining the valence state from the observed multiplet structure, which can be used as a fingerprint (van der Laan and Thole, 1991; van der Laan and Kirkman, 1992). In this respect, the nearly filled d shell of Cu compounds is almost too simple, since for $d^9 \rightarrow \underline{2p}d^{10}$ only a single peak is observed, and for d^{10} no peak is present because a formal $2p \rightarrow 3d$ transition is not possible. The presence of a very sharp peak at a photon energy close to 931 eV in the L_3 XAS is a common feature for all divalent Cu compounds (Grioni et al., 1989; van der Laan et al., 1992). In contrast to $2p$ XPS, the final state in L_3 XAS is effectively screened by the additional $3d$ electron excited from the $2p$ core shell. This leads to a final state $\underline{2p}3d^{10}$, which for CuO is at 931.2 eV, 2 eV below the XPS main ($\underline{2p}3d^{10}L$) peak (Fig. 2a). In the reported divalent Cu minerals (Grioni et al., 1989; van der Laan et al., 1992) the L_3 peak position is found in a very narrow energy range (between 930.5 and 931.2 eV) and the L_3 peak is very sharp, due to the absence of hybridization in the final state $\underline{2p}3d^{10}$ configuration. The small energy shift of the XAS peak is due to changes in the ground-state hybridization, crystal-field splitting and Madelung energy for the different minerals.

Monovalent Cu compounds display a completely different behaviour (Grioni et al., 1989; van der Laan et al., 1992; van der Laan et al., 2002; Patrick et al., 2004). Com-

pared to divalent compounds, the main peak is shifted towards higher photon energy, as expected from the electrostatic potential. Compared to the corresponding $2p$ XPS main peak, the L_3 XAS main peak is at lower energy for CuO (Fig. 2a), at higher energy for Cu₂O (Fig. 2b), but at approximately the same energy for CuFeS₂ (Fig. 2c). If the XAS main peak is assigned to $2p^5 3d^{10} s$, it might be expected that its energy position should reflect the energy of the unoccupied s state. However, the energy position bears little relationship to the band gap (Table 2), hence the situation seems to be more complicated, and the precise nature of the peaks in Cu L_3 XAS is more ambiguous than in the $2p$ XPS. The peaks are close together so that they are expected to have mixed character. From the description of the electronic structure of the monovalent Cu compounds described above, it is clear that the ground state is, in general, predominantly d^{10} with some $d^9 s$ character and is mixed with ligand $d^{10} \underline{L}_s$ character (Grioni et al., 1992). Similar to Cu₂O, the L_3 XAS of CuFeS₂ shows a relatively intense peak at the onset (Fig. 2b and c). The experimental spectrum of Cu₂O is in good agreement with a Clogston–Wolff impurity model calculation where the asymmetric line shape of the main peak arises from the core hole effect (Grioni et al., 1992). In CuFeS₂ the main peak is more symmetric. The intense peak in the L_3 XAS of both CuFeS₂ and Cu₂O is considerably broader than the peak in the L_3 XAS of CuO, suggesting stronger final-state hybridization.

The cross-section for X-ray absorption from the $2p$ to the $4s$ state is weaker than that from the $2p$ to the $3d$ state. Patrick et al. (1993) found that the intensity of the main peak in chalcopyrite is 25 times weaker than in CuO. This means that contamination by small amounts of nominally Cu²⁺ components will be easily observed in spectra of nominally monovalent minerals, as shown in Fig. 2b and f. It is sometimes stated that the $2p$ to $4s$ transitions can be neglected, because its cross-section is small (de Groot, 2005). However, this is not a good approximation when the number of d holes is small, as is the case for Cu. Consider a ground-state Ψ_g that has mixed character, i.e., $|\psi_g\rangle = \alpha|d^{10}\rangle + \beta|d^9 s\rangle$, where α^2 and β^2 are the probabilities of the d^{10} and $d^9 s$ configurations in the ground state. Both these configurations can reach the same final state $2p^5 d^{10} s$ configuration by $2p \rightarrow 4s$ and $2p \rightarrow 3d$ transitions, respectively. The intensity is given by $(\alpha D_s + \beta D_d)^2$, where D_s and D_d are the amplitudes for the transitions from $2p$ to $4s$ and from $2p$ to $3d$, respectively. For $D_d \gg D_s$ this gives an intensity equal to $\beta^2 D_d^2 + 2\alpha\beta D_d D_s$, where the sec-

ond term becomes relevant for $\alpha \gg \beta$, i.e., monovalent compounds. Hence the transitions to the $4s$ state cannot be ignored.

3.4. Fe $L_{2,3}$ XAS

As stated above for Fe $2p$ XPS, the Fe site is unlikely to have an integer d count. It is not possible to determine the d count from the Fe $L_{2,3}$ XAS in the same way as with Cu $L_{2,3}$ XAS, because the Cu²⁺ ion contains only a single d hole and the $d^9 \rightarrow 2p^5 3d^{10}$ transition gives a single peak at the L_3 edge, whereas the Fe ion has several d holes and the strong electrostatic interactions between these d holes in the ground state, as well as with core hole in the final state, make the Fe $L_{2,3}$ peaks broad. However, Fe $L_{2,3}$ XAS does provide a powerful tool for determining the local spin state of $3d$ transition Fe ions in their compounds, when combined with atomic multiplet calculations. Fig. 3 shows the Fe $L_{2,3}$ XAS spectra of chalcopyrite compared with some iron phases. The spectral structure is due to the transitions $2p^6 3d^n \rightarrow 2p^5 3d^{n+1}$. The Fe L_3 ($2p_{3/2}$) and L_2 ($2p_{1/2}$) multiplet structures are separated by a $2p$ spin-orbit splitting of 12.3 eV. The spectrum of chalcopyrite shows the characteristic structure for Fe³⁺ d^5 in a small crystal field (Fig. 3a). The shape of the Fe $L_{2,3}$ XAS for chalcopyrite resembles that of KFeS₂ (Fig. 3b) which is high-spin Fe³⁺ in a tetrahedral site ($10Dq = 0.5$ eV) (Atanasov et al., 1995). With an increasing crystal field, the weaker transition at the higher energy side of the L_3 structure disappears, while a low-energy shoulder grows in intensity, as is visible in hematite (Fe₂O₃, Fig. 3c), which has an octahedral crystal field of $10Dq = 1.8$ eV (van der Laan and Kirkman, 1992). The high-spin Fe²⁺ d^6 configuration, such as that of troilite (FeS, Fig. 3d), normally shows a double peak structure for the L_3 XAS (van der Laan and Kirkman, 1992). The low-spin Fe²⁺ configuration, such as that of pyrite (FeS₂, Fig. 3e), is characterised by a lower branching ratio, $L_3/(L_3 + L_2)$, compared to the high-spin configuration (Thole and van der Laan, 1988). Therefore, based on the shape of the spectra, Fe $L_{2,3}$ XAS provides strong evidence that the iron in chalcopyrite is high-spin Fe³⁺. However, as the charge difference between nominally Fe²⁺ and Fe³⁺ can be as low as 0.2 electrons, the relative energy difference between the configurations does not provide an accurate determination of the valency state. It is, therefore, necessary to use other spectroscopic techniques such as ⁵⁷Fe Mössbauer to provide more definitive evidence for the nominal valence state of Fe³⁺ in CuFeS₂.

3.5. ⁵⁷Fe Mössbauer spectroscopy

The Mössbauer spectrum of chalcopyrite consists of a six-line hyperfine magnetic spectrum arising from magnetically ordered iron in one position in the structure (see

Table 2
Energies for the XPS main peak, XAS main peak and optical band gap for selected Cu compounds (Folmer and Jellinek, 1980; van der Laan et al., 1981; Shen et al., 1987; Tjeng, 1990; Fujisawa et al., 1994)

Compound	XPS main peak (eV)	XAS main peak (eV)	Optical gap (XPS)
CuO	933.2	931.2	1.4
Cu ₂ O	932.4	933.8	2.17
CuFeS ₂	932.3	932.5	0.6

Marfunin and Mkrtchyan, 1967; Vaughan and Burns, 1972; Vaughan and Craig, 1978 for an overview). The isomer shift, which relates directly to *s* electron density at the nucleus and hence to shielding by the *d* electrons and to the ‘*d* count’, is small (0.20 mm s⁻¹ at 300 K, 0.27 mm s⁻¹ at 80 K) and this is characteristic of high-spin Fe³⁺. The quadrupole splitting which, if present, arises from asymmetry in the spatial distribution of electrons around the nucleus, is reported as zero or very small. This is as would be expected for such a symmetric species as Fe³⁺ in an undistorted site. (If present, the sixth *d* electron in Fe²⁺ would contribute to a significant quadrupole splitting.) The hyperfine field at the nucleus (350 kG at 300 K) is also consistent with high-spin Fe³⁺. It is important to note that these values are very different to those for Fe²⁺ in a similar environment. For example, iron-bearing sphalerite (ZnFe)S, where other measurements (e.g., optical absorption spectra) clearly show iron occurring as Fe²⁺, has a much larger isomer shift (0.66 mm s⁻¹ at 300 K) and quadrupole splitting (0.80 mm s⁻¹ at 300 K) consistent with this difference in oxidation state (Marfunin and Mkrtchyan, 1967). Stannite, where formal valencies must be Cu₂⁺Fe²⁺Sn⁴⁺S₄²⁻ and which is also isostructural with chalcopyrite, again has very different isomer shift (0.57 mm s⁻¹) and quadrupole splitting (2.84 mm s⁻¹) parameters to those for iron in chalcopyrite (see Vaughan and Burns (1972) and references therein). On the other hand, in bornite, where formal valencies dictate the presence of trivalent iron (Cu₅⁺Fe³⁺S₄²⁻), reported isomer shifts (0.39 mm s⁻¹) and quadrupole splittings (0.16 or 0 mm s⁻¹) (Marfunin and Mkrtchyan, 1967; Vaughan and Burns, 1972) fall, like those of chalcopyrite, in a range consistent with the Fe³⁺ valence state. The experimental Mössbauer data for chalcopyrite, when compared with data for other sulfide minerals (as reviewed in Vaughan and Craig, 1978) clearly point to formal valence states of Cu⁺Fe³⁺S₂²⁻.

4. Discussion

Chalcopyrite has all the characteristics of a formally monovalent Cu compound, with the defining criteria being the absence of the 2*p* satellite in XPS and the L₃ XAS lacking a single sharp peak around 931 eV but showing a broader structure at higher energy. The work of Todd and Sherman (2003) and Todd et al. (2003) has led to an erroneous interpretation of the XAS spectra of chalcopyrite where they claim a formal valency of Cu²⁺Fe²⁺S₂²⁻. This assumption is based on a simplistic comparison with the covellite (CuS) Cu *L*-edge spectrum which reveals similarity in energy of the first, low-energy peak in the chalcopyrite spectrum to a peak found in covellite, which they assume to be a Cu(II)/Cu(I) compound. Covellite, CuS, is indeed a compound in which Cu²⁺ might be expected if normal charge balance is assumed (as Cu₂⁺S : Cu²⁺S₂) but its first peak is at 932.0 eV (Fig. 2) and it falls into the nominally monovalent class without evidence of a rec-

ognisable Cu²⁺ component as has recently been confirmed by Goh et al. (2006). Todd et al. (2003) use the comparison of the Fe *L*-edge spectra of chalcopyrite to that of mackinawite (FeS) to conclude the iron to be divalent. However, the XPS, XAS and Mössbauer data presented here support the Cu⁺Fe³⁺S₂²⁻ configuration. Furthermore, mackinawite is a poor model for high-spin Fe²⁺ in sulfides, as its magnetic and electrical properties (Pauli paramagnetism, metallic conductivity) are inconsistent with this interpretation of the electronic configuration of the iron. Todd et al. (2003) also used an XAS study of the chalcopyrite surface obtained during oxidation in air-saturated aqueous solution (pH 2–10) to imply the formal valencies of Cu²⁺Fe²⁺S₂²⁻. They found that the copper component of chalcopyrite remained relatively unchanged during aqueous oxidation, suggesting that the copper was already present as oxidised Cu²⁺, whereas the Fe *L*-edges showed a marked change, suggesting that the iron was present as Fe²⁺ and was then oxidised to Fe³⁺. However, many previous investigations (Vaughan et al., 1995; Yin et al., 1995, 2000) have demonstrated that moderate oxidation of the chalcopyrite surface produces only Cu⁺ sulfide species together with Fe³⁺ oxides overlying a metal-depleted sulfide layer. Therefore, the changes observed in the Fe *L*-edge spectra can be explained by a transition from an Fe³⁺ sulfide to an Fe³⁺ oxide, forming a surface layer. This transition also results in a reduction in intensity of the Cu *L*-edge spectrum at pH 10.27 (Todd et al. (2003, Figs. 3–4)). The lack of change in the Cu *L*-edge spectra is also entirely consistent with this interpretation as Cu is retained at the surface as a Cu⁺ sulfide in these early stages of oxidation.

Nominally divalent character in copper sulfides is very rare (see above). Peaks around 931.0 eV are recorded in the published spectra of some Cu-sulfides that can be explained by (often minor) contamination by Cu²⁺ species, e.g., CuFeS₂ (Sainctavit, 1989; Sainctavit et al., 1990) and CuS (Todd et al., 2003). Contamination of CuO is also observed in Cu₂O spectra (van der Laan et al., 1992; Patrick et al., 1993; Todd and Sherman, 2003) and is responsible for the small peak (peak 1, Fig. 2b) in the Cu₂O spectrum presented here. For comparison with the pure CuS spectrum (Fig. 2g), a CuS sample with a small Cu²⁺ contamination is shown (Fig. 2f) which results in a characteristic lower-energy peak (peak 3, Fig. 2f). The relative intensity ratio of 25:1 for the Cu²⁺:Cu⁺ contributions means that even very small amounts of Cu²⁺ will have a large effect on the spectra of Cu⁺ phases. The tetrahedrite group minerals, ((Cu₁₀⁺Me₂²⁺)₁₂(Sb, As)₄³⁺S₁₃²⁻) have, however, been shown to incorporate a ‘genuine’ minor Cu²⁺ component in compositions deficient in other divalent metals such as Zn or Fe such that divalent Cu²⁺ is required for charge neutrality. This Cu²⁺ is manifest as a peak at 930.6 eV (peak 2, Fig. 2d) and can be contrasted to that in a tetrahedrite mineral (goldfieldite) with a composition of Cu₁₀Te₄S₁₃ which has no charge balance requirement for Cu²⁺ (Fig. 2e) (Patrick et al., 1993).

Recently published work in this area (Mikhlin et al., 2005), citing the studies by Todd and Sherman (2003) and Todd et al. (2003), perpetuates the erroneous interpretation of a formal valency of $\text{Cu}^{2+}\text{Fe}^{2+}\text{S}_2^{2-}$ for chalcopyrite. Although Mikhlin et al. (2005) are in agreement that the formal Cu valence is between 1+ and 2+ and is dominated by the 1+ component, the assignment of a 3+ valency for Fe is called into question. It is worth noting that, apart from clear cut cases such as hematite (Fe_2O_3), the Fe $L_{2,3}$ -edge XAS does not always provide an immediate verification of the valency state. It is, therefore, necessary to corroborate the Fe $L_{2,3}$ XAS data with complementary spectroscopic techniques such as ^{57}Fe Mössbauer and XPS, as described in this paper.

5. Conclusions and wider implications

In order to characterise the oxidation state of copper and iron in covalent compounds containing Cu and Fe, it is necessary to identify them as being formally monovalent or divalent for Cu, and as formally divalent or trivalent for Fe. Cu $2p$ XPS and Cu L -edge XAS spectra are invaluable tools for undertaking this task, with respect to Cu, by revealing information about the d^9/d^{10} count, contributing to an understanding of the electronic structure of the minerals, and to the nature of their covalent bonding. The determination of the valency and d count of Fe is not as straightforward and requires the use of further complementary techniques such as ^{57}Fe Mössbauer spectroscopy. From analysis using this range of techniques, it is clear that the formal valency formula for chalcopyrite is $\text{Cu}^+\text{Fe}^{3+}\text{S}_2^{2-}$. The assignment of the correct valence states for Cu and Fe in chalcopyrite is necessary to understand and predict its behaviour in a range of different areas including copper mineral processing, materials science and geochemistry. The determination of the electronic structure of chalcopyrite is fundamental to understanding the redox processes associated with copper ore beneficiation and is also essential for its applications as a semiconducting material (along with related phases such as CuFeSe_2 and CuInSe_2). In the area of geochemistry, metal oxidation states in minerals are often assumed to be integral, whereas the effective oxidation state of the metal can be intermediate. Techniques for the high precision measurement of Cu isotopes have recently been developed which require the correct assignment of charge on complex molecular species. Fractionations (mineral–fluid; mineral–mineral) are often measured experimentally avoiding possible problems of using calculated fractionation curves. However, for Cu-species where fractionations are calculated, or where experimental and calculated data show discrepancies, the actual d count can be an important consideration. The presence of variable oxidation states and measurable stable isotopic ratios in both Cu and Fe means that Cu/Fe-bearing species have an untapped potential to provide insights into processes

operating during the condensation of the solar nebula in the solar system and during the evolution of the Earth. In addition, the processes that link inorganic and biological chemistry in low-temperature environments, where redox elements such as Cu and Fe play an important role, require the reliable assignment of copper and iron oxidation states in order to develop meaningful interpretations.

Acknowledgments

The authors are very grateful to Drs. Ian Kirkman, Andy Smith and Mark Roper of CCLRC Daresbury for their assistance with the experiments. We also thank Dr. John Charnock for his continuing support of environmental-related XAS.

Associate editor: Liane G. Benning

References

- Atanasov, M., Potze, R.H., Sawatzky, G.A., 1995. Electronic structure of tetrahedral iron(III)-sulfur clusters in alkaline thioferrates: an X-ray absorption study. *J. Solid State Chem.* **119**, 380–393.
- Chen, C.T., Idzerda, Y.U., Lin, H.J., Smith, N.V., Meigs, G., Chaban, E., Ho, G.H., Pellegrin, E., Sette, F., 1995. Experimental confirmation of X-ray magnetic circular dichroism, sum-rules for iron and cobalt. *Phys. Rev. Lett.* **75**, 152–155.
- de Groot, F., 2005. Multiplet effects in X-ray spectroscopy. *Coord. Chem. Rev.* **249**, 31–63.
- Donnay, G., Corliss, L.M., Donnay, J.D.H., Elliot, N., Hastings, J.M., 1958. Symmetry of magnetic structures: magnetic structure of chalcopyrite. *Phys. Rev. B* **112**, 1917–1923.
- Edelbro, R., Sandström, A., Paul, J., 2003. Full potential calculations on the electron band structures of Sphalerite, Pyrite and Chalcopyrite. *Appl. Surf. Sci.* **206**, 300–313.
- Folmer, J.C.W., Jelinek, F., 1980. The valence of copper in sulphides and selenides: an X-ray photoelectron spectroscopy study. *J. Less Common Metals* **76**, 153–162.
- Fujisawa, M., Suga, S., Mizokawa, T., Fujimori, A., Sato, K., 1994. Electronic structures of CuFeS_2 and $\text{CuAl}_{0.9}\text{Fe}_{0.1}\text{S}_2$ studied by electron and optical spectroscopies. *Phys. Rev. B* **49**, 7155–7164.
- Goh, S.W., Buckley, A.N., Lamb, R.N., 2006. Copper(II) sulfide? *Miner. Eng.* **19**, 204–208.
- Griani, M., Goedkoop, J.B., Schoorl, R., de Groot, F.M.F., Fuggle, J.C., Schäfers, F., Koch, E.E., Rossi, G., Esteva, J.-M., Karnatak, R.C., 1989. Studies of copper valence states with Cu L_3 X-ray absorption spectroscopy. *Phys. Rev. B* **39**, 1541–1545.
- Griani, M., van Acker, J.F., Czyzyk, M.T., Fuggle, J.C., 1992. Unoccupied electronic structure and core-hole effects in the X-ray-absorption spectra of Cu_2O . *Phys. Rev. B*.
- Hamajima, T., Kambara, T., Gondaira, K.I., Oguchi, T., 1981. Self-consistent electronic structures of magnetic semiconductors by a discrete variational X- α calculation. III. Chalcopyrite CuFeS_2 . *Phys. Rev. B* **24**, 3349–3353.
- Karlsson, K., Gunnarsson, O., Jepsen, O., 1992a. Chemical shifts for monovalent, divalent and trivalent Cu compounds. *J. Phys.: Condens. Matter* **4**, 895–909.
- Karlsson, K., Gunnarsson, O., Jepsen, O., 1992b. Shape of the Cu $2p$ core level photoemission spectrum for monovalent, divalent and trivalent Cu compounds. *J. Phys.: Condens. Matter* **4**, 2801–2816.
- Kurmaev, E.Z., van Ek, J., Ederer, D.L., Zhou, L., Callcott, T.A., Perera, R.C.C., Cherkashenko, V.M., Shamin, S.N., Trofimova, V.A., Bartkowski, S., Neumann, M., Fujimori, A., Moloshag, V.P., 1998.

- Experimental and theoretical investigation of the electronic structure of transition metal sulphides: CuS, FeS₂ and FeCuS₂. *J. Phys.: Condens. Matter* **10**, 1687–1697.
- Marfunin, A.S., Mkrtychyan, A.R., 1967. Mössbauer spectra of iron-57 in sulfide minerals. *Geokhimiya* **10**, 1094–1103.
- Mikhlin, Y., Tomashevich, Y.V., Tauson, V., Vyalikh, D.V., Molodtsov, S., Szargan, R., 2005. A comparative X-ray absorption near-edge structure study of bornite, Cu₅FeS₄ and chalcopyrite, CuFeS₂. *J. Electron Spectrosc. Relat. Phenom.* **142**, 83–88.
- Mikhlin, Y.L., Tomashevich, Y.V., Asanov, I.P., Okotrub, A.V., Varnek, V.A., Vyalikh, D.V., 2004. Spectroscopic and electrochemical characterization of the surface layers of chalcopyrite (CuFeS₂) reacted in acidic solutions. *Appl. Surf. Sci.* **225**, 395–409.
- Nakai, I., Sugitani, Y., Nagashima, K., 1978. X-ray photoelectron spectroscopic study of copper minerals. *J. Inorg. Nucl. Chem.* **40**, 789–791.
- Patrick, R.A.D., van der Laan, G., Charnock, J.M., Grguric, B.A., 2004. Cu L_{2,3} X-ray absorption spectroscopy and the electronic structure of minerals: spectral variations in non-stoichiometric bornites, Cu₅FeS₄. *Am. Mineral.* **89**, 541–546.
- Patrick, R.A.D., van der Laan, G., Henderson, C.M.B., Kuiper, P., Dudzik, E., Vaughan, D.J., 2002. Cation site occupancy in spinel ferrites studied by X-ray magnetic circular dichroism: developing a method for mineralogists. *Eur. J. Mineral.* **14**, 1095–1102.
- Patrick, R.A.D., van der Laan, G., Vaughan, D.J., Henderson, C.M.B., 1993. Oxidation state and electronic configuration determination of copper in tetrahedrite group minerals by L-edge X-ray absorption spectroscopy. *Phys. Chem. Miner.* **20**, 395–401.
- Saintavit, P., 1989. Ph.D Thesis, University of Paris VII.
- Saintavit, P., Petiau, J., Flank, A.-M., Ringeisen, J., Lewonczuk, S., 1990. Influence of 3d electrons at the Fermi level on the electronic densities of empty states in CuFeS₂, CuGaS₂, ZnS. In: *2nd European Conference on Progress in X-ray Synchrotron Radiation Research*.
- Shen, Z.X., Allen, J.W., Yeh, J.J., Kang, J.-S., Ellis, W., Spicer, W., Lindau, I., Maple, M.B., Dalichaouch, Y.D., Torikachvili, M.S., Sun, J.Z., Geballe, T.H., 1987. Anderson Hamiltonian description of the experimental electronic structure and magnetic interactions of copper oxide superconductors. *Phys. Rev. B* **36**, 8414–8428.
- Thole, B.T., van der Laan, G., 1988. Branching ratio in X-ray absorption spectroscopy. *Phys. Rev. B* **38**, 3158–3171.
- Tjeng, L.H., 1990. Ph.D. Thesis, University of Groningen.
- Todd, E.C., Sherman, D.M., 2003. Surface oxidation of chalcocite (Cu₂S) under aqueous (pH 2–11) and ambient atmospheric conditions: Mineralogy from Cu L- and O K-edge X-ray absorption spectroscopy. *Am. Mineral.* **88**, 1652–1656.
- Todd, E.C., Sherman, D.M., Purton, J.A., 2003. Surface oxidation of chalcopyrite (CuFeS₂) under ambient atmospheric and aqueous (pH 2–10) conditions: Cu, Fe L- and O K-edge X-ray spectroscopy. *Geochim. Cosmochim. Acta* **67**, 2137–2146.
- Tossell, J.A., Urch, D.S., Vaughan, D.J., Wiech, G., 1982. The electronic structure of CuFeS₂, chalcopyrite, from X-ray emission and X-ray photoelectron spectroscopy and X- α calculations. *J. Chem. Phys.* **77**, 77–82.
- van der Laan, G., Kirkman, I.W., 1992. The 2p absorption spectra of 3d transition metal compounds in tetrahedral and octahedral symmetry. *J. Phys.: Condens. Matter* **4**, 4189–4204.
- van der Laan, G., Patrick, R.A.D., Charnock, J.M., Grguric, B.A., 2002. Cu L_{2,3} X-ray absorption and the electronic structure of non-stoichiometric Cu₅FeS₄. *Phys. Rev. B* **66**, 045104-1-5.
- van der Laan, G., Patrick, R.A.D., Henderson, C.M.B., Vaughan, D.J., 1992. Oxidation state variations in copper minerals studied with Cu 2p X-ray absorption spectroscopy. *J. Phys. Chem. Solids*, 53.
- van der Laan, G., Thole, B.T., 1991. Strong magnetic X-ray dichroism in 2p absorption spectra of 3d transition metal ions. *Phys. Rev. B* **43**, 13401–13411.
- van der Laan, G., Westra, C.H., Sawatzky, G.A., 1981. Satellite structure in photoelectron and Auger spectra of copper dihalides. *Phys. Rev. B* **23**, 4369–4380.
- Vaughan, D.J., Burns, R.G., 1972. Mössbauer spectroscopy and bonding in sulphide minerals containing four-coordinated iron. In: *Proceedings of the 24th International Geological Congress*, Section 14, pp. 158–167.
- Vaughan, D.J., Craig, J.R., 1978. *Mineral Chemistry of Metal Sulphides*. Cambridge University Press, Cambridge, MA.
- Vaughan, D.J., England, K.E.R., Kelsall, G.H., Yin, Q., 1995. Electrochemical oxidation of chalcopyrite (CuFeS₂) and the related metal-enriched derivatives Cu₄Fe₃S₈, Cu₉Fe₉S₁₆ and Cu₉Fe₉S₁₆. *Am. Mineral.* **80**, 725–731.
- Vaughan, D.J., Ridout, M.S., 1971. Mössbauer Studies of some sulphide minerals. *J. Inorg. Nucl. Chem.* **33**, 741–746.
- Velasquez, P., Leinen, D., Pascual, J., Ramos-Barrado, J.R., Cordova, R., Gomez, H., Schrebler, R., 2001. XPS, SEM, EDX, and EIS study of an electrochemically modified electrode surface of natural chalcocite. (Cu₂S). *J. Electroanal. Chem.* **510**, 20–28.
- Yin, Q., Kelsall, G.H., Vaughan, D.J., England, K.E.R., 1995. Atmospheric and electrochemical oxidation of the surface of chalcopyrite (CuFeS₂). *Geochim. Cosmochim. Acta* **59**, 1091–1100.
- Yin, Q., Vaughan, D.J., England, K.E.R., Kelsall, G.H., Brandon, N.P., 2000. Surface oxidation of chalcopyrite (CuFeS₂) in alkaline solutions. *J. Electrochem. Soc.* **147**, 2945–2951.